Climate Dynamics
https://doi.org/10.1007/s00382-024-07110-8

ORIGINAL ARTICLE

# Interdecadal variation of tropical cyclone genesis longitudes over the western North Pacific

JaeWon Choi[1,3] · Kyong-Hwan Seo[1,2,3]

Received: 15 March 2023 / Accepted: 9 January 2024
© The Author(s), under exclusive licence to Springer-Verlag GmbH Germany, part of Springer Nature 2024

**Abstract**
Statistical change-point analysis was used to examine a significant change in the average longitude locations of tropical cyclone (TC) genesis from June to October between 1979 and 2020. It was observed that since 1998, the TC genesis location has shifted westward. This study investigates the causes of this interdecadal shift in the western North Pacific (WNP). During the recent period (1998–2020), a westward shift was noted in precipitation, outgoing longwave radiation, precipitable water, and total cloud cover. The primary driver for this shift is the negative phase of the Pacific Decadal Oscillation during the second period. A positive sea surface temperature (SST) anomaly enhances convection over the South China Sea and adjacent waters west of 140° E, which retreats the monsoon trough toward the west. Furthermore, the Rossby wave response to a negative SST anomaly over the central and eastern Pacific causes the WNP subtropical high in the lower troposphere to move further west, pushing the monsoon trough in the same direction. The westward shifts in convection and circulation are maintained by a strengthened Walker circulation.

**Keywords** Tropical cyclone · Pacific Decadal Oscillation · Western North Pacific subtropical high · Walker circulation

## 1 Introduction

The western North Pacific (WNP) is the water body where tropical cyclone (TC) activity is the most active on Earth. The TCs that occur in these waters migrate west to affect southern China or Vietnam or north to affect the mid-latitude region of East Asia. The regions affected by TCs are mostly determined by the location of TC genesis (Wang and Chan 2002). The TCs that occurred in the southeastern waters of the WNP migrate northwest and recurve in the East China Sea and eventually affect East Asia. As these TCs travel long distances over the ocean, they gain sufficient energy from the ocean to generate higher intensity and affect the mid-latitude region of East Asia. Meanwhile, TCs that occur in the northwestern waters of the WNP generally migrate short distances to the west to affect southern China and Vietnam. These TCs generally have low intensity because of the topographical effect of the Philippines (Wang and Chan 2002; Choi et al. 2010).

Studies have focused on the tendency of TCs to occur over the western part of the WNP and have revealed that the tropical upper-tropospheric trough (TUTT), monsoon trough, and El Niño-Southern Oscillation (ENSO) affected WNP TC genesis locations (Huang et al. 2016; Wang and Wu 2016; Huangfu et al. 2017; Deng et al. 2018). Huang et al. (2017) attributed the westward shift of the TUTT to the recent westward migration of the monsoon trough. Hu et al. (2018) recently reported that more TCs tended to occur in the northwestern part of the WNP and showed that this was related to a shift in convective anomalies for El Niño-Southern Oscillation (ENSO) and a climate regime shift in the Pacific Ocean in 1998. Through observational data analysis and model simulations, Cao et al. (2020) suggested that changes to the La Niña-type Pacific sea surface temperature (SST), which induced the recent global warming hiatus, are responsible for the northwest migration of the location of the WNP TC genesis.

It is well known that SST is an important environmental factor influencing TC activity. In a study on the relationship

✉ Kyong-Hwan Seo
khseo@pusan.ac.kr

[1] BK21 School of Earth and Environmental Systems, Pusan National University, Busan, Republic of Korea

[2] Department of Atmospheric Sciences, Pusan National University, Geumjeong-Gu, Busan 46241, Republic of Korea

[3] Research Center for Climate Sciences, Pusan National University, Busan, Republic of Korea

Published online: 17 February 2024

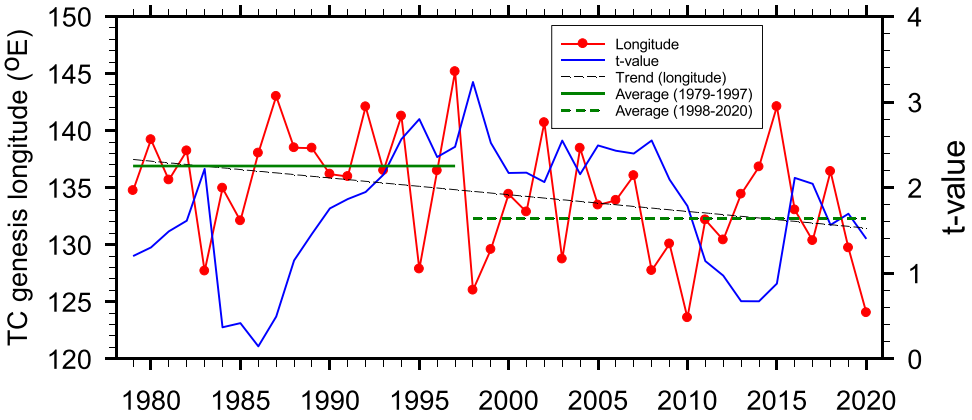


**Fig. 1** Time series of TC genesis longitude averaged for June–October (JJASO) (red line with dot) and the statistical change-point profile (blue line)

between Pacific Decadal Oscillation (PDO) and TC, Lee et al. (2021) indicated that the frequency of TCs passing through Korea and Japan during the negative phase of PDO increased by approximately 50%, compared to those in the positive phase. Wang and Liu (2016) investigated how PDO modulates the effect of ENSO on the rapid intensification (RI) of TCs in the WNP. The relationship between ENSO and RI frequency was shown to be statistically significant in the warm PDO phase. Scoccimarro et al. (2021) showed that PDO modulates TC days in the North Pacific Ocean. In addition, many other studies have investigated the association between TC activity and PDO (Zhou et al. 2007; Kubota and Chan 2009; Liu and Chan 2008, 2013; Yang et al. 2018).

There are some papers on the westward shift of the WNP TC genesis location. Wu et al. (2015) stressed that a pronounced westward shift in the TUTT is found in all of the available reanalysis data sets during 1979–2012, suppressing TC genesis in the eastern portion (east of 145° E) of the western North Pacific basin due to the enhanced vertical wind shear associated with the TUTT shift. As a result, the annual mean TC genesis longitude had significantly shifted westward since 1979. Cao et al. (2020) suggested that there is consensus on the causes for the northwestwards shift of autumn TC genesis positions over the WNP after the late 1990s. They further examined the interdecadal change of the TC genesis position over the WNP during September–November (SON) after the late 1990s based on the composite analysis and a suite of atmospheric general circulation model (AGCM) experiments. Feng and Wu (2022) showed that the basin-wide mean location of TC formation shifted northward in the western North Pacific (WNP) basin over the past four decades. Here they focused on the interdecadal variability of the monsoon trough (MT), within which most TCs in the WNP basin occur, and its roles in the shift of the basin-wide mean location of TC formation using 60-year reanalysis data. However, each study has a different mechanism for the westward shift of the TC Genesis location. Therefore, we analyze the relationships between the westward shift of the WNP TC genesis location during peak TC season (June–October) and the PDO on the decadal timescale.

In Sect. 2, the data and methodology are shown, and a time series of TC genesis longitude locations is analyzed in Sect. 3. In Sect. 4, the recent westward shift of the WNP TC genesis location and atmospheric circulations is analyzed. In Sect. 5, the effect of SST variation on the recent westward shift of the WNP TC genesis location is analyzed. The results of this study are summarized in Sect. 6.

## 2 Data and methodology

### 2.1 Data

The best-track data of the Regional Specialized Meteorological Center–Tokyo Typhoon Center were used as the TC data. In this study, Reanalysis-2 (R-2) monthly average data of the National Center for Environmental Prediction–Department of Energy were used (Kanamitsu et al. 2002). These data consist of 2.5° × 2.5° latitude–longitude grid spacing with a total of 17 vertical layers from 1979 to 2020. Extended Reconstructed Sea Surface Temperature (ERSST) V3b (Smith et al. 2008) data were used as the SST data. ERSST data are the monthly averages from 1854 to the present and consist of 2° × 2° grid spacing. Outgoing longwave radiation (OLR) data were also analyzed (Liebmann and Smith 1996). The University of Washington (http://jisao.washington.edu/pdo) provides PDO index (Mantua et al. 1997).

### 2.2 Methodology

The vertical wind shear (VWS) was calculated as the method of Wingo and Cecil (2010).

The VWS for the diagnosis of the large-scale condition is calculated as follows:

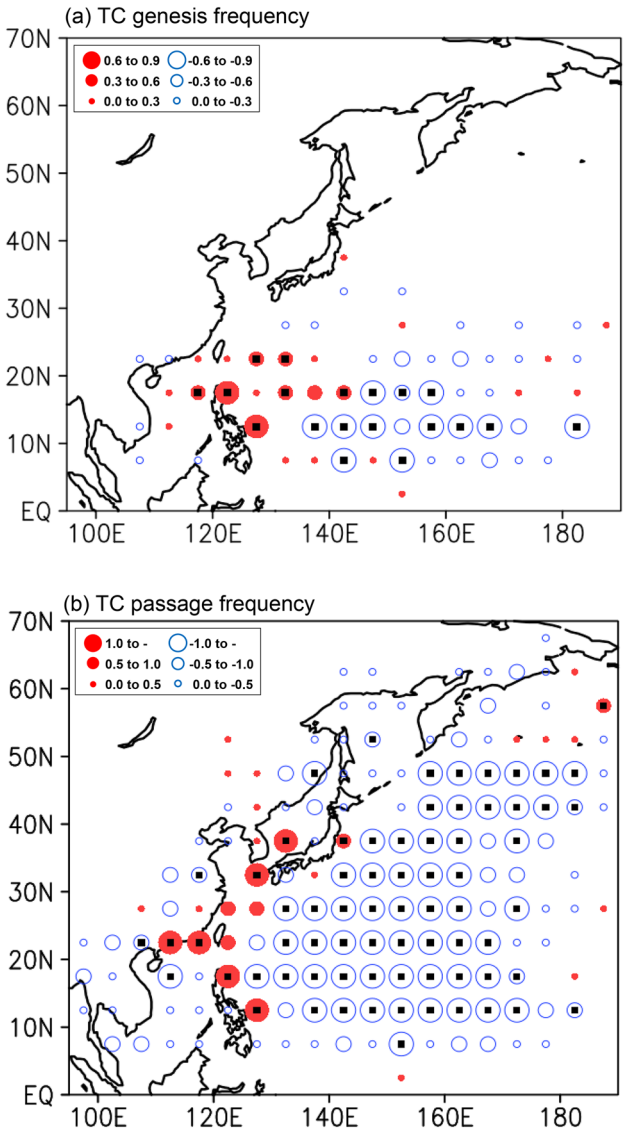


**Fig. 2** Differences in **a** TC genesis frequency (TCGF) and **b** TC passage frequency (TCPF) between 1998–2020 and 1979–1997 in JJASO. In **a**, **b**, the small squares inside the circles indicate that the differences are significant at the 95% confidence level. *TC* tropical cyclone. Legends indicate that mean TC genesis frequency (**a**) and TC passage frequency (**b**) on the differences between 1998–2020 and 1979–1997 in JJASO

$$VWS = \sqrt{\left(u_{200} - u_{850}\right)^2 + \left(v_{200} - v_{850}\right)^2}.$$

Here, $u$ and $v$ indicate the zonal and meridional winds, respectively. 200 and 850 represent 200-hPa and 850-hPa levels. The genesis potential index (GPI) is defined from the equation of Camargo et al. (2007). To determine the significance of the results, the two-tailed Student's $t$ test was used (Wilks 1995).

The Walker circulation index is defined as the difference in 500-hPa omega velocities between the eastern equatorial Pacific (160° W–80° W, 5° S–5° N) and the western (80° E–160° E, 5° S–5° N) equatorial Pacific (Vecchi et al. 2006).

In order to calculate TC passage frequencies, each TC was calculated after being relocated within a 5°×5° grid. Even if a TC passed over the same grid multiple times, it was regarded as a single passage. TC genesis frequencies were also calculated by the above manner.

## 3 Westward shift of TC genesis longitude since 1998

Figure 1 shows the time series of TC genesis longitude averaged during June–October for 1979–2020 (red line with dots). This time series has distinct interannual and interdecadal variations. Therefore, a statistical change-point analysis was applied to this time series (blue line) using a 9-year sliding window. The largest absolute value of the $t$-value appears in 1998, indicating a shift in the climate regime around this year. The average longitude of TC genesis was 136.9° E during 1979–1997 and 132.3° E during 1998–2020, with a difference of 3.6° between the two periods. This difference was significant at the 95% confidence level. This implies that TCs occurred farther west by approximately 300–400 km during 1998–2020 than during 1979–1997. In the next section, the average difference between the periods 1998–2020 and 1979–1997 is analyzed to determine why more recent TCs have occurred farther west of the WNP than before.

## 4 Large-scale environment and atmospheric circulation

First, we analyzed the difference in TC genesis frequency between the two periods (Fig. 2a). TCs during 1998–2020 had a strong tendency to occur mainly in the sea near the Philippines and in the South China Sea. However, during 1979–1997, TCs had a higher preference in the eastern waters of the WNP. That is, recently, TCs occurred more often to the western side of the WNP. However, there ar e still dots over the Asian lands. This is because when TC genesis is placed at a grid box of 5°×5°, it seems that TC genesis also appeared on land in East Asia. The TC passage frequency indicates that the frequency of TC migration along the East Asian coast is higher (Fig. 2b); therefore, East Asian coastal countries have an increased TC-related risk.

The reason why recent TCs have occurred west of the WNP can be found from the GPI field (Fig. 3a). A positive anomaly was located in the northern region as well as in the western region of the WNP. Conversely, a negative anomaly

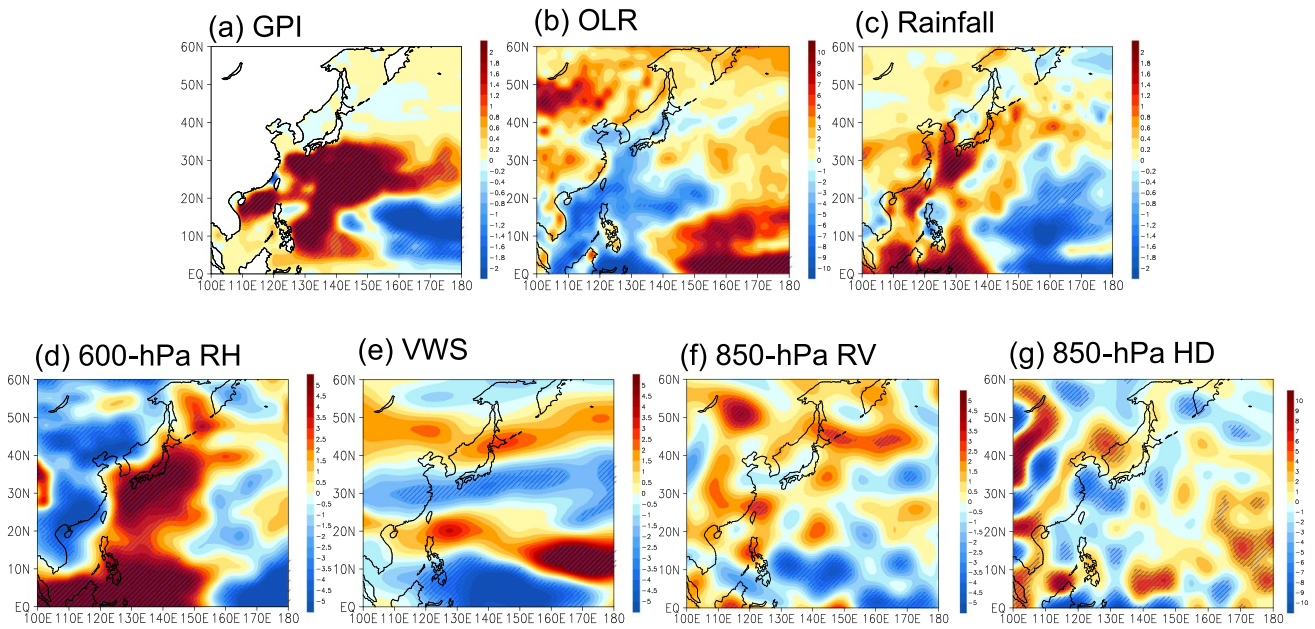


**Fig. 3** Composite differences in **a** GPI, **b** OLR, **c** rainfall, **d** 600-hPa relative humidity (RH), **e** vertical wind shear (VWS), **f** 850-hPa relative vorticity, and **g** 850-hPa horizontal divergence between 1998–2020 and 1979–1997 in JJASO. Hatched areas are significant at the 95% confidence level

was located south of 20° N and east of 150° E. As a proxy for deep convection, OLR is shown in Fig. 3b where a negative OLR anomaly is distributed in the western region of the WNP (relative to 140° E), and a positive anomaly is in the eastern part of the WNP. This means that during 1998–2020, convection was more active in the western WNP than during 1979–1997. The precipitation field indicates a spatial distribution opposite to that of the OLR (Fig. 3c); the region west of 140°E shows the positive anomaly, while the region east of 140°E shows the negative anomaly.

The occurrence of TCs in more or less farther western area of the WNP during 1998–2020 can also be attributed to environmental factors affecting the occurrence of TCs. For example, the 600-hPa relative humidity (RH600) shows that the region west of 150° E has a positive anomaly, while the region east of 150°E has a negative anomaly (Fig. 3d). The VWS field shows that the negative anomaly south of 10° N is located farther west than the positive anomaly at 10°–20° N (Fig. 3e). Figure 3f shows a positive low-level relative vorticity anomaly located slightly farther northwest than the negative anomaly in the WNP. The 850-hPa horizontal divergence shows anomalous convergence over the western region of the WNP, while anomalous divergence over the eastern region of the WNP (Fig. 3g). All these indicate that convection during 1998–2020 is more active in the west of the WNP than during 1979–1997.

To examine whether the climate regime shift occurred in 1998 in all of the above variables, statistical change-point analysis for GPI, OLR, and RH600 was applied to the area-averaged time series in the western (0°–25° N, 100°–140° E) and eastern regions (0°–25° N, 140°–180° E) of the WNP (Fig. 4), where 140° E is the longitude of dividing the opposite anomalies in the OLR field (Fig. 3b). Trends for GPI and RH600 averaged in the western WNP shows an increasing trend, but OLR shows a decreasing trend (these trends were significant at the 95% confidence level), indicating that the large-scale environment favorable for the occurrence of TCs in the western region of the WNP has formed in recent years. The statistical change-point applied to the time series reveals that the largest absolute value of the *t*-value existed for 1998 for all three variables. Thus, the supportive environments for the formation of TCs have been present in the western WNP since 1998. Meanwhile, environments unfavorable for the occurrence of TCs have been formed in the eastern WNP (the area-averaged GPI and RH600 decreased, while OLR increased). This region also shows the largest absolute value of the *t*-value occurring in 1998, indicating that fewer TCs have occurred in the eastern region of the WNP since 1998.

The changes in the large-scale environments, shown above, between 1998–2020 and 1979–1997 can be identified in the difference in the 850-hPa winds between the two periods (Fig. 5a). Whereas the large anomalous anticyclonic circulation exists in the WNP region, an anomalous cyclonic circulation is located near Lake Baikal. This is the west-low–east-high spatial pressure pattern. Owing to the huge anomalous anticyclonic circulation located in the WNP during 1998–2020, TCs could not develop in the eastern

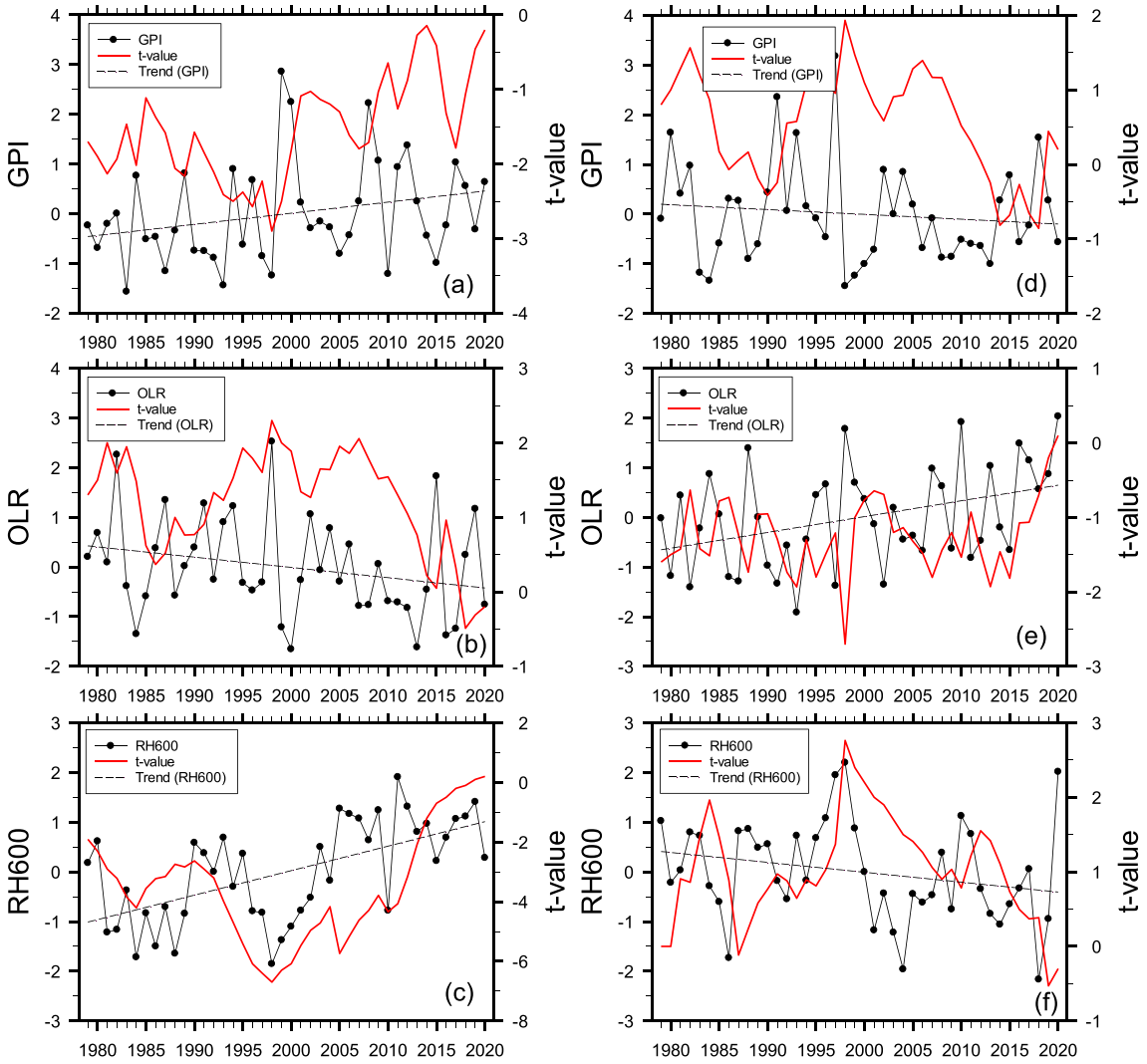


**Fig. 4** Time series of GPI, OLR, 600-hPa RH averaged for the western area (0°–25° N, 100°–140° E; left panel) and the eastern area (0°–25° N, 140°–180° E; right panel) of the western North Pacific in JJASO

WNP but rather occurred in the western WNP. In addition, from this anomalous pressure pattern, the eastern coast of China and the Korean peninsula are affected by anomalous southerlies; these steering flows affect the TC track shown in Fig. 2b, in such a way that during 1998–2020, TCs could mainly affect the Korean Peninsula from the Philippines region through the east coast of China. The tendency for TCs to occur to the west during 1998–2020 was identified in the longitudinal position of monsoon troughs in the two periods (represented by red lines in Fig. 5b, c). The monsoon trough appeared only up to 125° E during 1998–2020 (Fig. 5b) but expanded eastward to approximately 140° E during 1979–1997 (Fig. 5c); the latter situation supports the development of TC to more eastern side of the WNP.

In above section, we analyzed that convection is more active in the western WNP but less convection in the eastern WNP based on 140°E. To identify characteristics of the vertical flows, we analyze meridional circulation based on 140°E. For the latitudinal range of 100°–140° E, the meridional circulation pattern (left panel of Fig. 6a) shows the anomalous upward motions over the region where TCs mainly occur (0°–28° N), whereas the anomalous downward motions are formed in the mid-latitude zone of East Asia (30°–40° N); in contrast, for the domain of 140°–180° E, the anomalous downward motions develop strongly at 5°–20° N, while anomalous upward motions are formed at 20°–40° N (right panel of Fig. 6a). This property is also manifested in the longitude–height plot (Fig. 6c). The relative humidity anomalies (Fig. 6b) shows roughly the consistent result with other variables. These atmospheric circulations and moisture

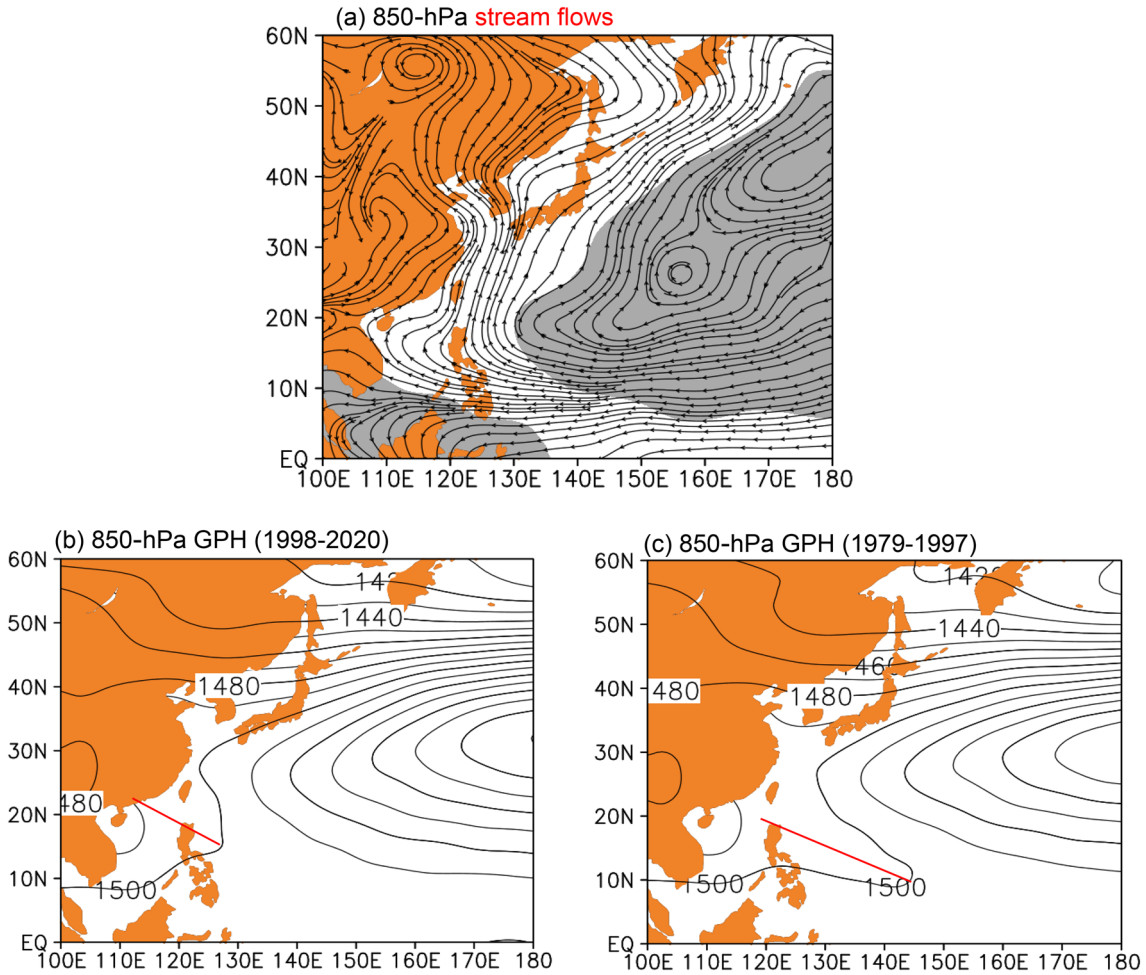


**Fig. 5** **a** Composite difference in stream flows at 850-hPa between 1998–2020 and 1979–1997 in JJASO and composites of **b** 850-hPa geopotential height (GPH) for 1998–2020 and **c** 850-hPa GPH for 1979–1997 in JJASO. In **a**, gray-shaded areas are significant at the 95% confidence level

conditions are directed toward the formation of more TCs in the western region of the WNP during 1998–2020.

The TUTT is an elongated trough stretching from the mid-latitude to the tropics (red lines in Fig. 7a, b) and since it induces a large amount of VWS, tropical disturbances can be subdued. However, in the vicinity of TC center (usually to the northeast of it), TUTT can help ventilate the upper-level air so that TC can develop and/or intensify (Barry and Carleton 2001). The mean east–west shift of the TUTT is measured with the dividing boundary between the easterly and westerly winds in the trough (the zero contour of zonal wind speed over 5° N–20° N) (Wu et al. 2015). Figure 7a, b show evidently that the TUTT developed westward to 155° E during 1998–2020 but contracted eastward to 165° E during 1979–1997, indicating the favorable environment for more TCs to develop over western WNP. The longitudinal location of the TUTT averaged in June–October was analyzed each year (Fig. 7c). The longitudinal location of the TUTT shows a decreasing trend, which is significant at the 95% confidence level. There is a clear in-phase relationship between the locations of the TC genesis and TUTT longitudes; a positive correlation of 0.62 (0.59 if the linear trends are removed) was found between the two variables. The statistical change-point analysis (Fig. 7d) shows that the largest absolute value of the *t*-value occurred in 1998, indicating the interdecadal variation of the TUTT longitudes.

## 5 Teleconnection related to SST variation

The difference in SST between the two periods (Fig. 8a) indicates a warm anomaly over the western region of the WNP and a cold one over the eastern region. This spatial distribution of SST anomalies causes TCs during 1998–2020 to occur in the western WNP. In fact, the whole SST field is typical of the cold PDO pattern and its index shows a

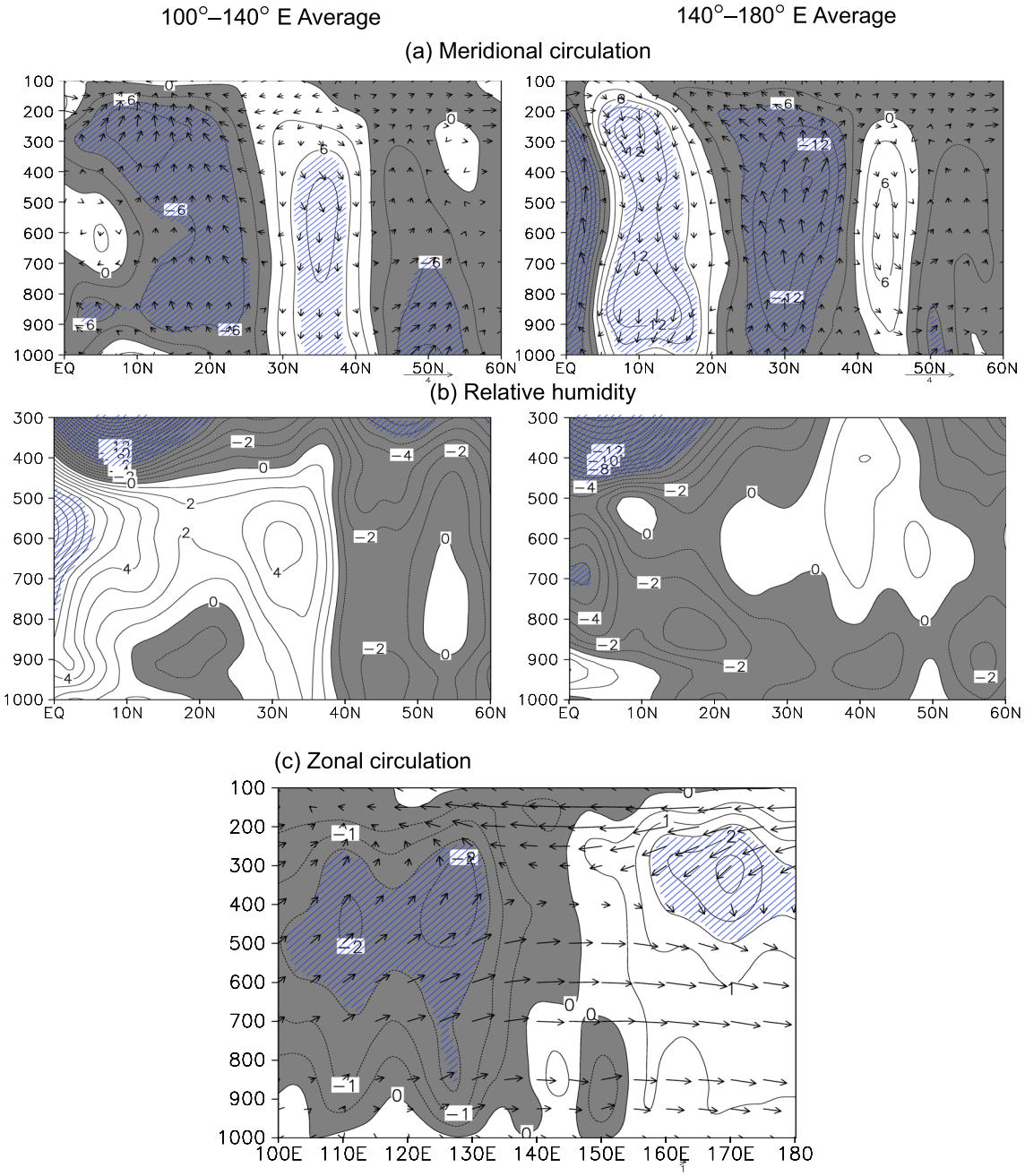


**Fig. 6** Composite differences of latitude–pressure cross-section of **a** vertical velocity (contours; hPa $s^{-1}$) and meridional circulation (vectors), **b** relative humidity (%) averaged along 100°–140° E (left panel) and 140°–180° E (right panel) between 1998–2020 and 1979–1997 in JJASO. **c** Denotes zonal circulation averaged along 0°–30° E between 1998–2020 and 1979–1997 in JJASO. The values of vertical velocity are multiplied by − 100. Hatched areas are significant at the 95% confidence level, and shaded areas denote negative values. Contour intervals are $3^{-2}$ hPa $s^{-1}$ and 1% for vertical velocity and relative humidity, respectively

decreasing trend until recently (Fig. 8b). This PDO time series has a correlation of 0.52 (0.49 if the linear trends are removed) with that of TC genesis longitudes averaged from June to October. This implies that the lower (higher) the PDO index is, the more TCs are formed in the western (eastern) region of the WNP. The statistical change-point analysis (Fig. 8c) demonstrates the largest absolute value of the *t*-value in 1998, indicating the interdecadal variation of the PDO index time series.

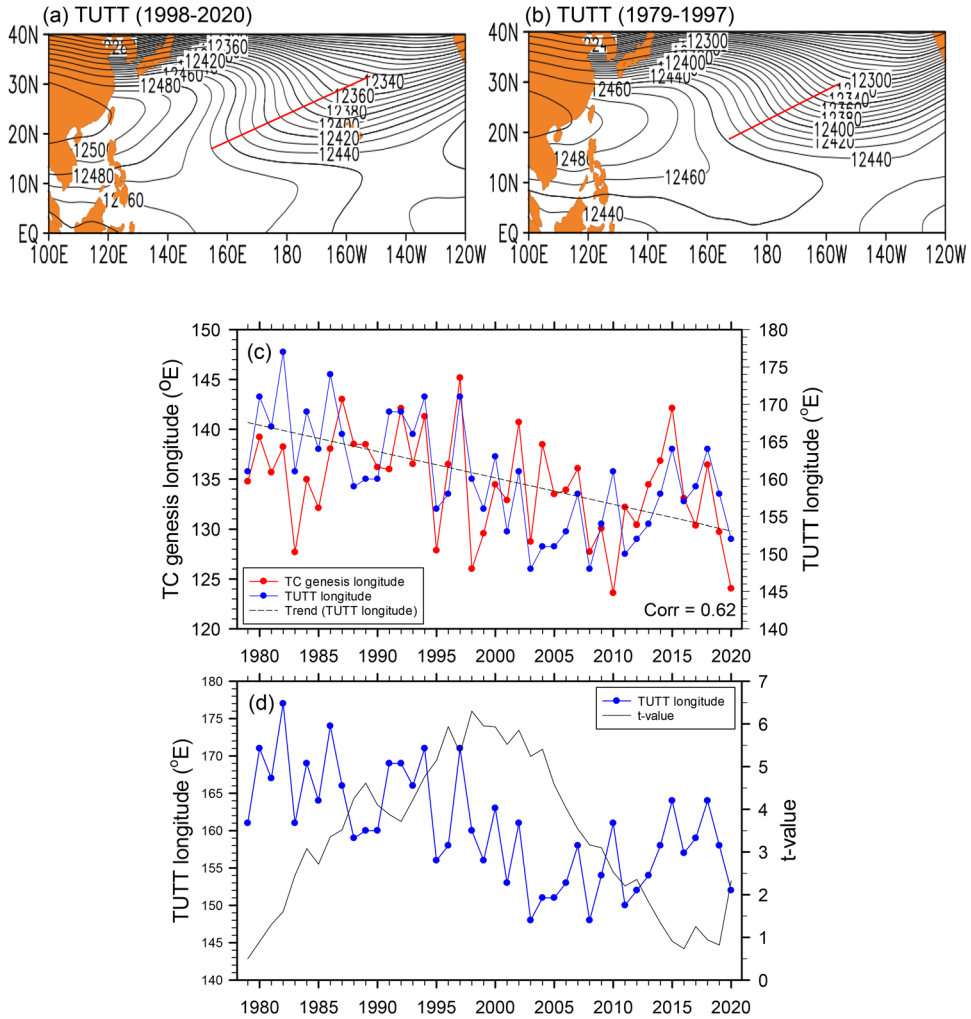


**Fig. 7.** 200 hPa geopotential height (gpm) to show tropical upper tropospheric trough (TUTT) averaged for **a** 1998–2020 and **b** 1979–1997 in JJASO and time series of **c** TC genesis longitude, TUTT longitude, and **d** t-value of the TUTT longitude

The difference in 500-hPa omega between the two periods (Fig. 9a) indicates the similar result. Over the latitudinal area of 0°–10° N, anomalous upward motions developed west of 160° E, while anomalous downward motions east of 160° E, implying the environment supportive of the formation of more TCs in the western WNP. The dipole pattern exhibits the strengthening of the Walker circulation after 1998. To examine whether Walker circulation is correlated with the location of TC genesis longitude, the average Walker circulation index during June–October is obtained by using the method of Vecchi et al. (2006). This index shows the increasing trend until recently, but this trend is not statistically significant (Fig. 9b). In addition, an out-of-phase relationship between the two variables was clear ($r = -0.68$), implying that the stronger (weaker) the Walker circulation is, the higher the possibility is of TCs occurring on the western (eastern) side of the WNP. The Walker circulation index also produces the largest *t*-value at 1998, as before. La Nina-like SST pattern (PDO) is found to shift the monsoon trough and tropical upper-tropospheric trough westward and thus leads to unfavorable large-scale conditions in the eastern WNP but favorable large-scale conditions in the western WNP. In other words, the phase change of the PDO can strengthen the Walker circulation and consequently shift the TC genesis westward.

## 6 Summary

The statistical change-point analysis was applied to the TC genesis longitude averaged from June to October from 1979–2020. It was found that the longitude of TC genesis has shifted to the west since 1998. The average longitude location during 1979–1997 was 136.9° E, whereas it was

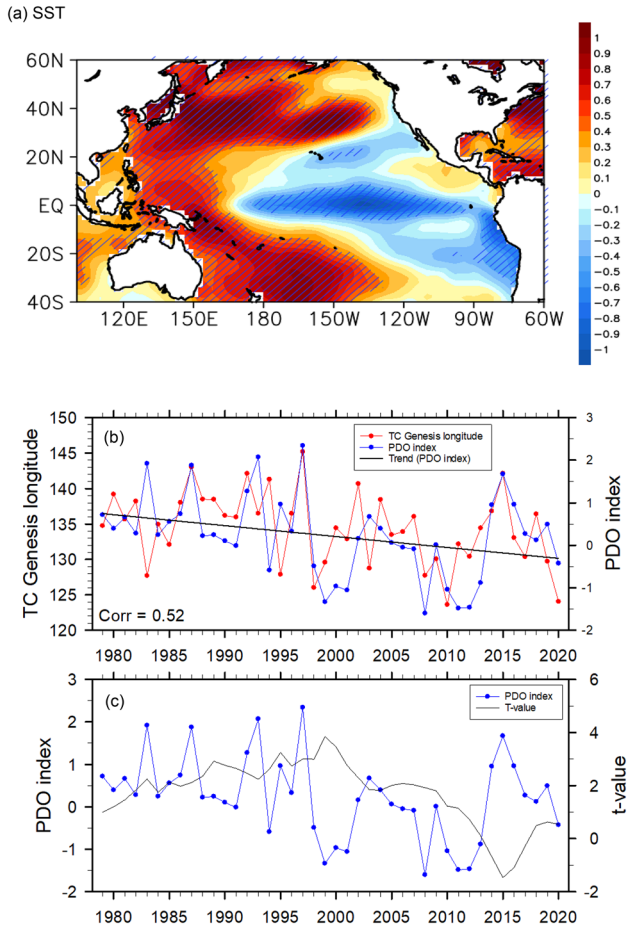


**Fig. 8** **a** Composite difference in SST between 1998–2020 and 1979–1997 in JJASO. Time series of **b** TC genesis longitude and Pacific Decadal Oscillation (PDO) index in JJASO and **c** *t*-value on PDO index. In **a**, hatched areas are significant at the 95% confidence level. *SST* sea surface temperature, *TC* tropical cyclone

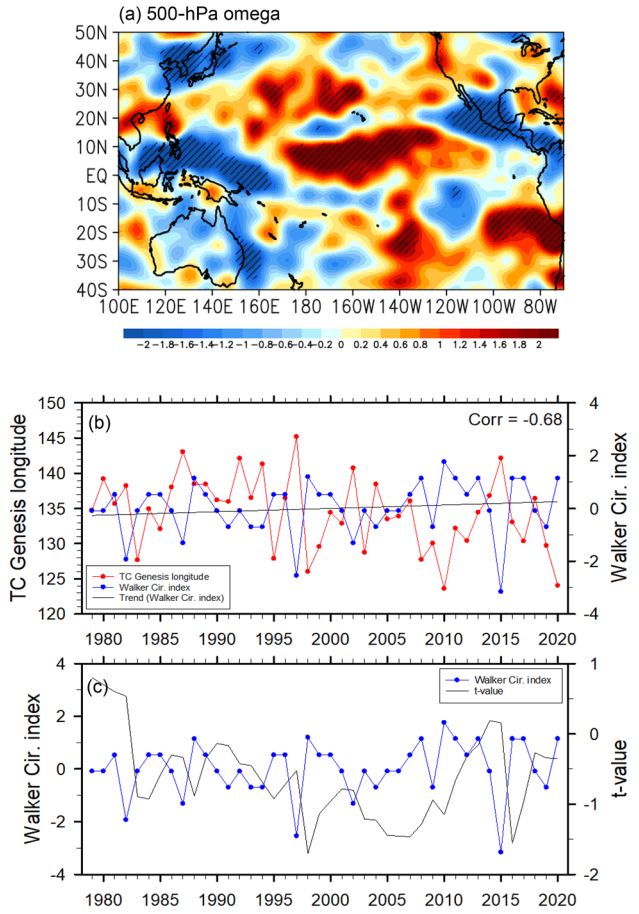


**Fig. 9** **a** Composite difference in 500-hPa omega in JJASO and time series of **b** TC genesis longitude and Walker circulation index and **c** *t*-value on Walker circulation index. In **a**, hatched areas are significant at the 95% confidence level. *TC* tropical cyclone

132.3° E during 1998–2020, a difference of 300–400 km in distance between the two periods. The present study investigates the possible mechanisms of this shift.

The recent trend for TCs occurring in the western WNP was confirmed by many thermodynamic and dynamics variables. Here, the positive precipitation, GPI, and 600-hPa relative humidity anomalies and negative OLR anomaly were observed in the western WNP, whereas the opposite signs of these variables appeared east of 140° E. All these indicate that convection was more active in the western area of the WNP during 1998–2020 than during 1979–1997. Other environmental factors are also favorable for the westward shift in the onset longitude of TC: a decrease (increase) in the VWS (850-hPa relative vorticity) anomaly over the western part of the WNP, a westward expansion of the WNPSH, and a westward retreat of the monsoon trough.

The primary driver for this shift is due mainly to the negative Pacific Decadal Oscillation (PDO) during the second period. A positive SST anomaly enhances convection over the South China Sea and adjacent waters west of 140°E, which retreats the monsoon trough toward the west. A flow chart summarizing the relevant processes is shown in Fig. 10.

This study showed that TC genesis longitude was shifted westward in the WNP during the cold PDO phase. The precise physical mechanisms can be verified using a series of sensitivity tests using coupled climate model, which will be pursued as a future work. As shown above, more TCs develop over the western area of the WNP in recent years, implying the higher risk of natural hazard along the coastal countries of East Asia, which requires increased precaution in those areas.

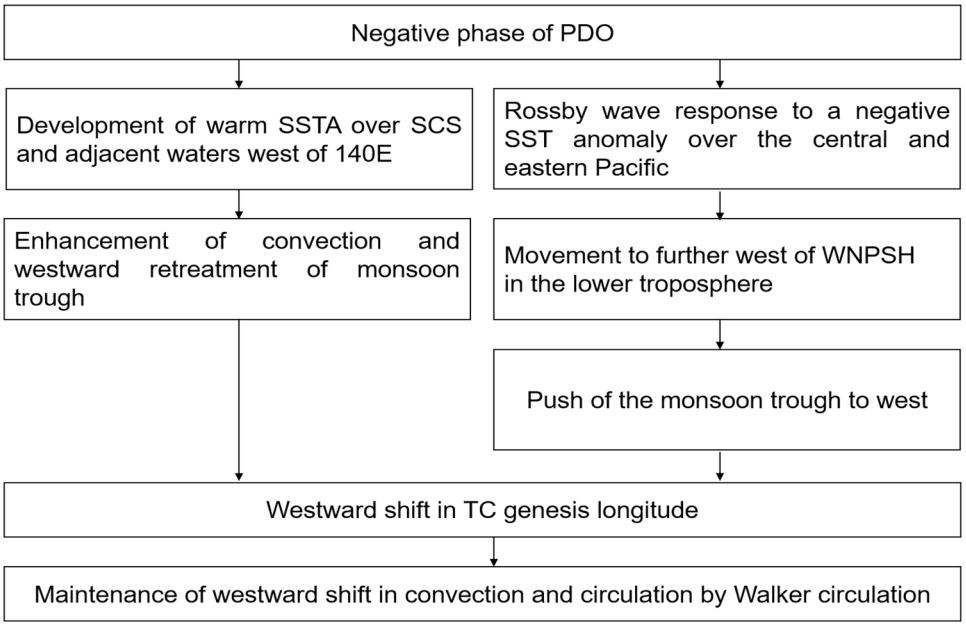


**Fig. 10** Flow chart of mechanism on westward shift of TC genesis longitude since 1998

**Author contributions** Conceptualization; JWC and K-HS, Methodology; JWC, Formal analysis and investigation; JWC, Visualization; Writing—original draft preparation; JWC and K-HS, Writing—review and editing; K-HS, Funding acquisition; K-HS, Supervision; K-HS.

**Funding** This work is supported by a National Research Foundation of Korea (NRF) grant funded by the Korean government (MSIP) (no. NRF-2020R1A2C2009414) and the Korea Meteorological Administration (KMA) Research and Development Program under Grant KMI2021-01410.

**Data availability** The best-track data produced by the Regional Specialized Meteorological Center–Tokyo Typhoon Center were used as the TC data. Reanalysis-2 (R-2) monthly average data distributed by the National Center for Environmental Prediction–Department of Energy were used. Extended Reconstructed Sea Surface Temperature (ERSST) V3b data were used as the SST data. The PDO index was obtained from the website of the University of Washington.

## Declarations

**Conflict of interest** The authors declare that they have no conflict of interest.

## References

Barry RG, Carleton AM (2001) Synoptic and dynamic climatology. Psychology Press, London, p 519

Camargo SJ, Emanuel KA, Sobel AH (2007) Use of a genesis potential index to diagnose ENSO effects on tropical cyclone genesis. IRI Technical Report 07-01. International Research Institute for Climate Prediction, Palisades, p 45

Cao X, Liu Y, Wu R, Bi M, Dai Y, Cai Z (2020) Northwestwards shift of tropical cyclone genesis position during autumn over the western North Pacific after the late 1990s. Int J Climatol 40:1885–1899

Choi KS, Wu CC, Cha EJ (2010) Change of tropical cyclone activity by Pacific-Japan teleconnection pattern in the western North Pacific. J Geophys Res 115:D19114. https://doi.org/10.1029/2010JD013866

Deng K, Yang S, Ting M, Hu C, Lu M (2018) Variations of the mid-Pacific trough and their relations to the Asian-Pacific-North American climate: roles of tropical sea surface temperature and Arctic sea ice. J Clim 31:2233–2252

Feng X, Wu L (2022) Role of interdecadal variability of the western North Pacific monsoon trough in shifting tropical cyclone formation. Clim Dyn 58:87–95

Hu C, Zhang C, Yang S, Chen D, He S (2018) Perspective on the northwestward shift of Autumn tropical cyclogenesis locations over the western North Pacific from shifting ENSO. Clim Dyn 51:2455–2465

Huang R, Huangfu J, Wu L, Feng T, Chen G (2016) Research on the interannual and interdecadal variabilities of the monsoon trough and their impacts on tropical cyclone genesis over the western North Pacific. J Tropic Meteorol 32:767–785 (**in Chinese**)

Huangfu J, Huang R, Chen W, Feng T, Wu L (2017) Interdecadal variation of tropical cyclone genesis and its relationship to the monsoon trough over the western North Pacific. Int J Climatol 37:3587–3596

Kanamitsu M, Ebisuzaki W, Woollen J, Yang SK, Hnilo JJ, Fiorino M, Potter GL (2002) NCEP-DOE AMIP-II Reanalysis (R-2). Bull Am Meteorol Soc 83:1631–1643

Kubota H, Chan JCL (2009) Interdecadal variability of tropical cyclone landfall in the Philippines from 1902 to 2005. Geophy Res Lett. https://doi.org/10.1029/2009gl038108

Lee M, Kim T, Cha DH, Min SK, Park DSR, Yeh SW, Chan JCL (2021) How does Pacific Decadal Oscillation affect tropical cyclone activity over Far East Asia? Geophy Res Lett 48:e2021GL096267

Liebmann B, Smith CA (1996) Description of a complete (interpolated) outgoing longwave radiation dataset. Bull Am Meteorol Soc 77:1275–1277

Liu KS, Chan JCL (2008) Interdecadal variability of western North Pacific tropical cyclone tracks. J Clim 21(17):4464–4476

Liu KS, Chan JC (2013) Inactive period of western North Pacific tropical cyclone activity in 1998–2011. J Clim 26(8):2614–2630
Mantua NJ, Hare SR, Zhang Y, Wallace JM, Francis RC (1997) A Pacific interdecadal climate oscillation with impacts on salmon production. Bull Am Meteorol Soc 78:1069–1079
Scoccimarro E, Villarini G, Gualdi S, Navarra A (2021) The Pacific decadal oscillation modulates tropical cyclone days on the interannual timescale in the North Pacific Ocean. J Geophy Res 126:e2021JD034988
Smith TM, Reynolds RW, Peterson TC, Lawrimore J (2008) Improvements to NOAA's historical merged land-ocean surface temperature analysis (1880–2006). J Clim 21:2283–2296
Vecchi GA, Soden BJ, Wittenberg AT, Held IM, Leetmaa A, Harrison MJ (2006) Weakening of tropical Pacific atmospheric circulation due to anthropogenic forcing. Nature 441:73–76
Wang B, Chan JCL (2002) How strong ENSO events affect tropical storm activity over the western North Pacific. J Clim 15:1643–1658
Wang X, Liu H (2016) PDO modulation of ENSO effect on tropical cyclone rapid intensification in the western North Pacific. Clim Dyn 46:15–28
Wang C, Wu L (2016) Interannual shift of the tropical upper-tropospheric trough and its influence on tropical cyclone formation over the western North Pacific. J Clim 29:4203–4211
Wilks DS (1995) Statistical methods in the atmospheric sciences. Academic Press, New York, p 467
Wingo MT, Cecil DJ (2010) Effects of vertical wind shear on tropical cyclone precipitation. Mon Weather Rev 138:645–662
Wu L, Wang C, Wang B (2015) Westward shift of western North Pacific tropical cyclogenesis. Geophys Res Lett 42:1537–1542
Yang L, Chen S, Wang C, Wang D, Wang X (2018) Potential impact of the pacific decadal oscillation and sea surface temperature in the tropical Indian Ocean-Western Pacific on the variability of typhoon landfall on the China coast. Clim Dyn 51(7):2695–2705
Zhou W, Li C, Wang X (2007) Possible connection between Pacific oceanic interdecadal pathway and East Asian winter monsoon. Geophy Res Lett. https://doi.org/10.1029/2006gl027809

**Publisher's Note** Springer Nature remains neutral with regard to jurisdictional claims in published maps and institutional affiliations.

Springer Nature or its licensor (e.g. a society or other partner) holds exclusive rights to this article under a publishing agreement with the author(s) or other rightsholder(s); author self-archiving of the accepted manuscript version of this article is solely governed by the terms of such publishing agreement and applicable law.